

# *The infrastructure for figures in INSPIRE*

Piotr Praczyk,

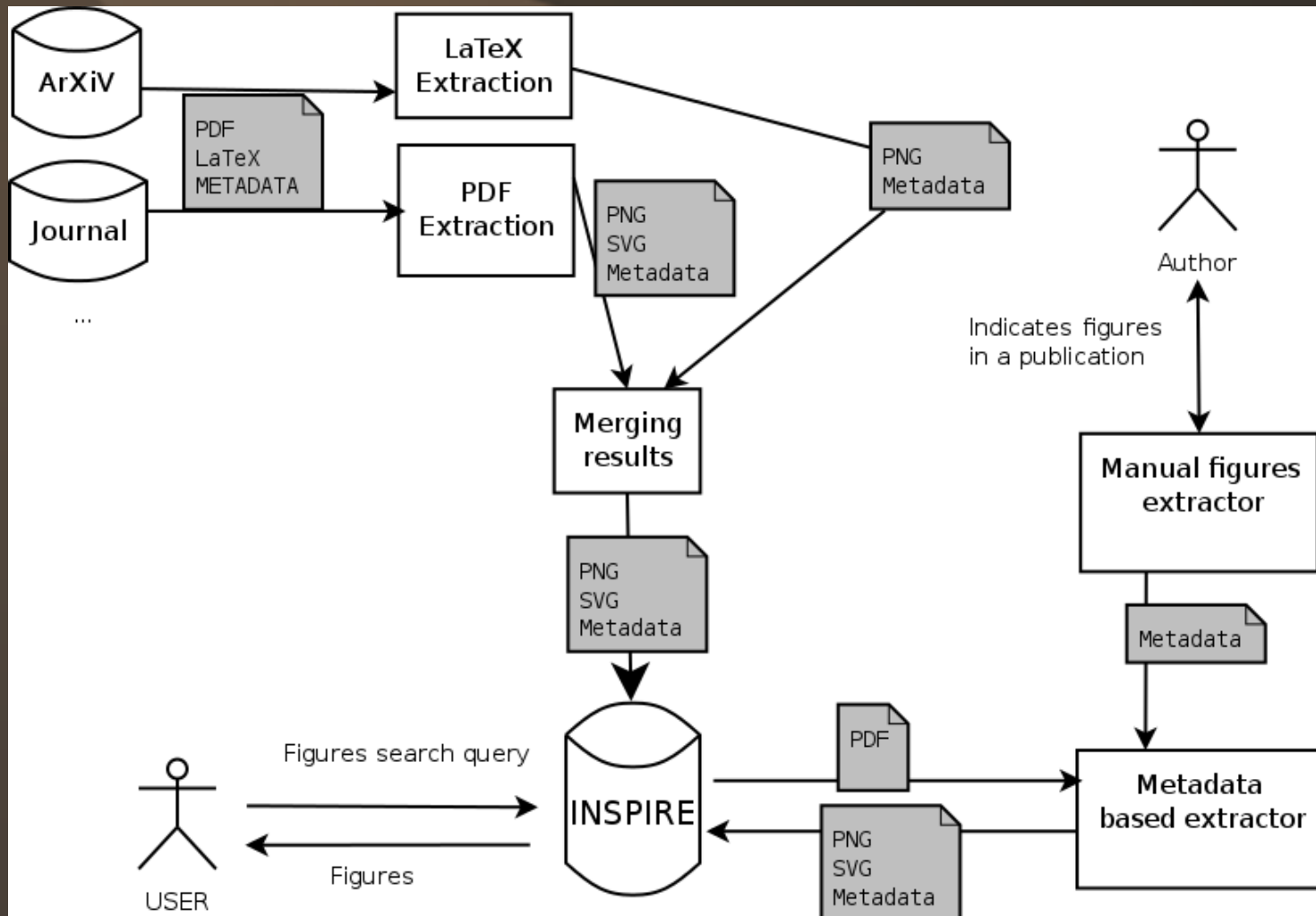
CERN 02/02/2012

# *Usage of graphics in scholarly communication*

- Describe experiments
- Summarise large amounts of data
- Illustrate relations between results
- Present ideas in a schematic manner



# Usage of Plots in Inspire



# Extracting data from PDF

PDF:

- Stream of instructions
- Embedded objects
  - Fonts
  - External objects
- Meta-description

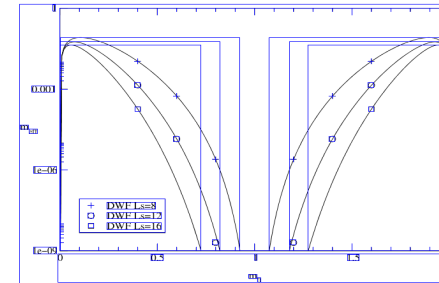


FIG. 1. Effective quark mass induced by domain-walls for the free field configuration.  $L_5$  is the number of lattice sites in the fifth direction

In the presence of a realistic gauge potential, the effective quark mass result from the finite wall separation may depend on how it is defined. Different definitions shall yield results consistent up to a factor of order unity. One approach is to exploit the explicit quark mass dependence in chiral Ward identities such as the Gell-Mann-Oakes-Renner (GMOR) relation as done in Ref. [7]. Here we explore the effective mass in an alternative way. In continuum field theory, the Atiyah-Singer theorem [8] states that the Dirac operator has a zero eigenvalue in the presence of an external background with topological charge  $|Q| \equiv 1$ . The explicit form of the solution was found by 't Hooft in 1976 [9]. On the lattice, however, the notion of topological charge is ill defined: any gauge configuration can be continuously deformed into a null gauge field. Moreover, the discretization of an instanton field can introduce finite lattice-spacing effects lifting any exact zero eigenvalue. Therefore, a test of the Atiyah-Singer theorem on lattice is usually complicated with various lattice artifacts.

There exists, however, a definition of lattice topology and fermion zero mode which largely avoids this complication. In the overlap formalism, the Dirac operator is constructed from the overlap of two many-fermion ground states [3]. According to their recipe, one starts from a four-dimensional Wilson-Dirac operator with a negative Wilson mass  $m_0$  and calculates its eigenvalues. For  $m_0$  small and positive, the number of positive eigenvalues is equal to that of negative ones. When  $m_0$  increases, a level might cross from positive to negative or vice versa. When this happens, the gauge field is regarded to have a net topological charge  $|Q| \equiv 1$ . Then the overlap determinant is exactly zero by construction. This definition of lattice topology and zero mode do depend on, for instance, the Wilson parameters  $r$  and  $m_0$ . However, the zero eigenvalue is exact, independent of the lattice spacing  $a$  and volume  $V$ .

# Intermediate steps of the algorithm

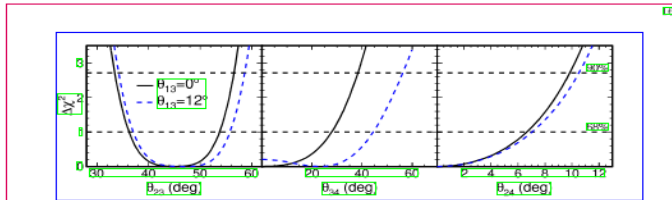


FIG. 14: Projections of  $\Delta\chi^2$  as a function of the mixing angles for the  $m_4 \gtrsim m_3$  model. The solid line is obtained for the case of null  $\nu_e$  appearance whereas the dashed line represents solutions with  $\nu_e$  appearance at the CHOOZ limit. The ranges of values allowed at 68% and 90% confidence levels lie within contours below the horizontal dashed lines.

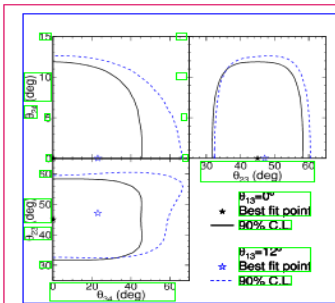


FIG. 15: Contours representing 90% confidence level for the  $m_4 \gtrsim m_3$  model. The solid line and best-fit point (solid symbol) are obtained for the case of null  $\nu_e$  appearance, whereas the dashed line and corresponding best-fit point (open symbol) is obtained with  $\nu_e$  appearance included with  $\theta_{13}$  at the CHOOZ limit.

Disappearance probability is a maximum. The determination of the limit follows the procedure described above but with the addition of selecting a value of  $\theta_{21}$  for each test case as well. At 90% confidence level  $f_s < 0.52$  (0.55 for  $E_\nu = 1.4$  GeV in this model). Thus, in either model, approximately 50% of the disappearing  $\nu_e$  can convert to  $\nu_\mu$  at 90% confidence level as long as the amount of  $\nu_e$  appearance is less than the limit presented by the CHOOZ collaboration.

## IX. OSCILLATIONS WITH DECAY

It was noted more than a decade ago that neutrino decay, as an alternative or companion process to neutrino oscillations, offers some capability for reproducing neutrino disappearance trends [18]. The model investigated here [36] includes neutrino oscillations occurring in parallel with neutrino decay. Normal neutrino-mass ordering is assumed, and the mass eigenstates  $\nu_1$ ,  $\nu_2$  are approximately degenerate, so that  $m_3 \gtrsim m_2 \approx m_1$ . The heaviest neutrino-mass state  $\nu_3$  is allowed to decay into an invisible final state. With these assumptions, and neglecting the small contributions from  $\nu_e$  mixing, only the two neutrino flavor states  $\nu_\mu$  and  $\nu_\tau$ , and the corresponding mass states  $\nu_2$  and  $\nu_1$ , are considered. The evolution of the neutrino flavor states is given by [36]:

$$\frac{d\psi}{dt} = \begin{pmatrix} -\frac{\Delta m_{21}^2}{4E} & -\cos 2\theta \sin 2\theta \\ \frac{\Delta m_{21}^2}{4E} & \cos 2\theta \sin 2\theta \end{pmatrix} \psi \quad (16)$$

where  $\tau_3$  is the lifetime of the  $\nu_3$  mass state and  $\theta$  is the mixing angle governing oscillations between  $\nu_\mu$  and  $\nu_\tau$ . Solving Eq. (16) one obtains probabilities for  $\nu_\mu$  survival or decay:

$$P_{\mu\mu} = \cos^4 \theta + \sin^4 \theta e^{-\frac{L}{\tau_3}} \quad (17)$$

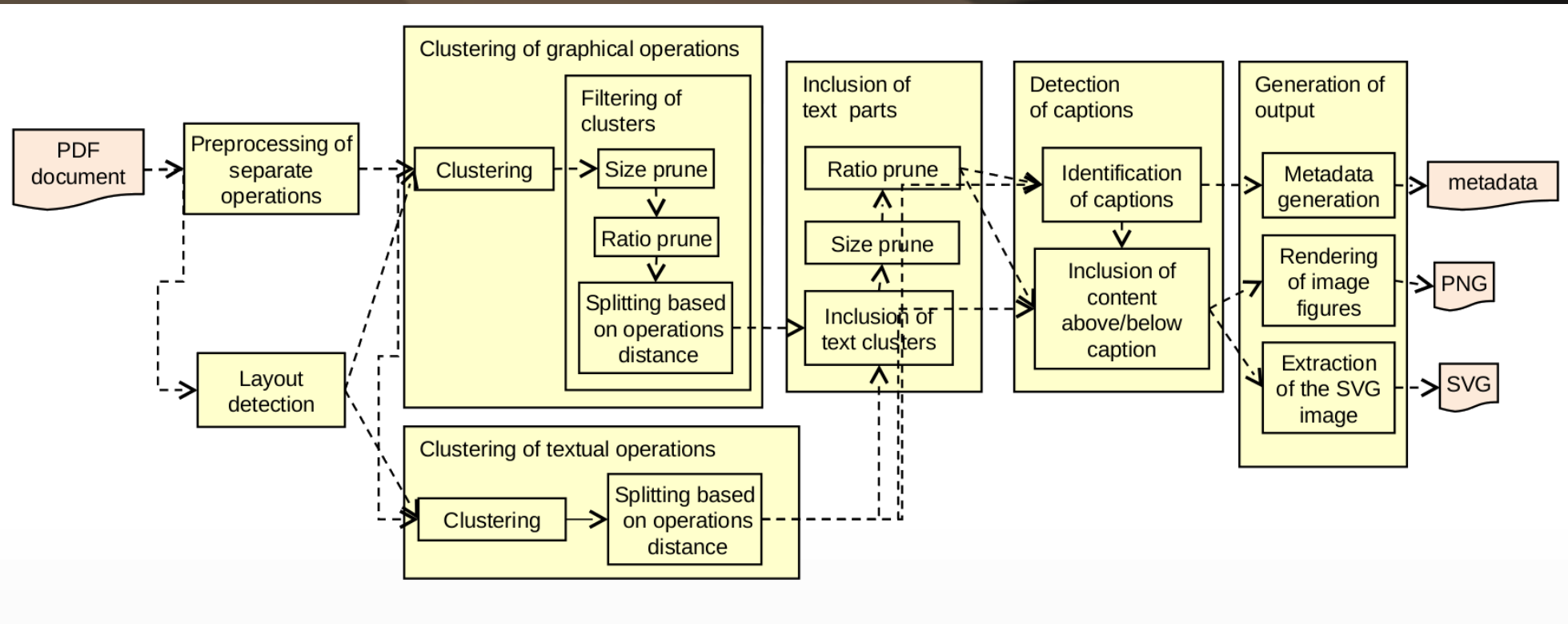
$$P_{\mu\tau} = 2 \cos^2 \theta \sin^2 \theta e^{-\frac{L}{\tau_3}} \cos \left( \frac{\Delta m_{21}^2 L}{2E} \right) \quad (18)$$

The limits  $\tau_3 \rightarrow \infty$  and  $\Delta m_{21}^2 \rightarrow 0$  correspond to a pure oscillations or a pure decay scenario, respectively.

In a conventional neutrino oscillations scenario, the ratio of the predicted charged-current spectrum in the far-detector with the null-oscillation expectation displays the characteristic “dip” at the assumed  $\Delta m_{21}^2$  value that is

- Regions of graphics (blue)
  - Clustered graphic operations
- Regions of text (green)
  - Clustered text operations
- Elements of page layout (red)

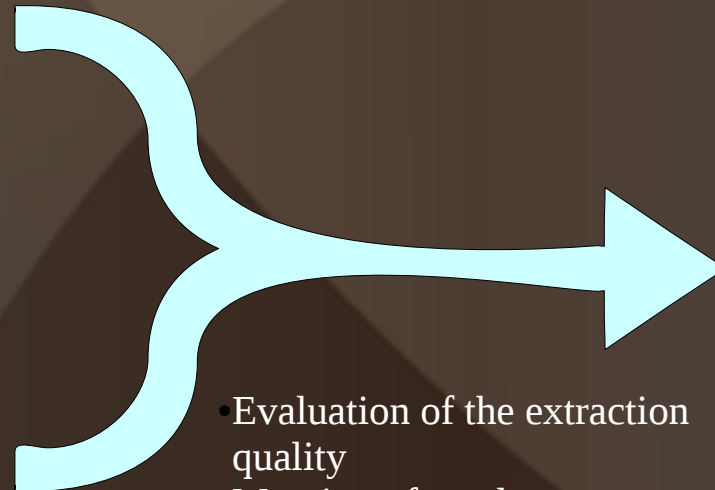
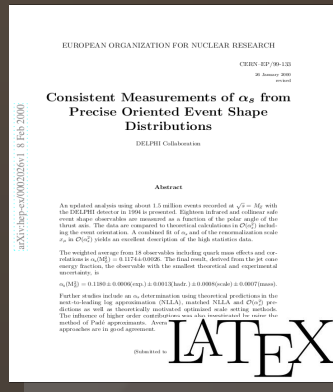
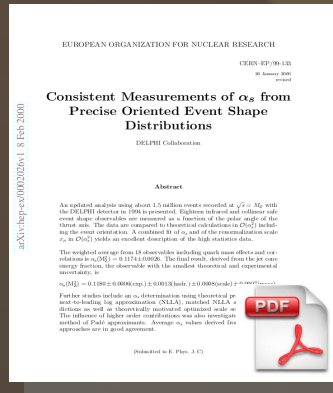
# *Extraction of figures from PDF*



# *LaTeX extraction*

- Most of documents are written using LaTeX
- Source file is parsed and attached figure files are converted to a standard format

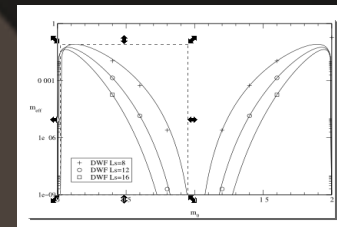
# Automatic extraction of figures



- Evaluation of the extraction quality
- Merging of results
- Acquisition of additional data

```
<scale>2</scale>
<pageResolution>
<width>1224</width>
<height>1584</height>
</pageResolution>
<pageNumber>0</pageNumber>
<pageCoordinates>
<x>269</x>
<y>168</y>
<width>682</width>
<height>494</height>
</pageCoordinates>
```

Meta-data



Vector + Raster images



(in the future)  
Semantic description



# *Types of extracted meta-data*

- Boundaries of figures
- Boundaries of captions
- Text of captions
- Graphics in PNG and SVG formats
- Places, where figure is referenced
- Name of the figure inside a document
- Text present inside the figure

# Select Your Figures

**Create new figure**

100%

FIG. 1. Effective quark mass induced by domain-walls for the free field configuration.  $L_5$  is the number of lattice sites in the fifth direction.

In the presence of a realistic gauge potential, the effective quark mass result from the finite wall separation may depend on how it is defined. Different definitions shall yield results consistent up to a factor of order unity. One approach is to exploit the explicit quark mass dependence in chiral Ward identities such as the Gell-Mann-Oakes-Renner (CMOR) relation as done in Ref. [7]. Here we explore the effective mass in an alternative way. In continuum field theory, the Atiyah-Singer theorem [8] states that the Dirac operator has a zero eigenvalue in the presence of an external background with topological charge  $|Q| = 1$ . The explicit form of the solution was found by 't Hooft in 1976 [9]. On the lattice, however, the notion of topological charge is ill defined: any gauge configuration can be continuously deformed into a null gauge field. Moreover, the discretization of an instanton field can introduce finite lattice-spacing effects lifting any exact zero eigenvalue. Therefore, a test of the Atiyah-Singer theorem on lattice is usually complicated with various lattice artifacts.

There exists, however, a definition of lattice topology and fermion zero mode which largely avoids this complication. In the overlap formalism, the Dirac operator is constructed from the overlap of two many-fermion ground states [3]. According to their recipe, one starts from a four-dimensional Wilson-Dirac operator with a negative Wilson mass  $m_0$  and calculates its eigenvalues. For  $m_0$  small and positive, the number of positive eigenvalues is equal to that of negative ones. When  $m_0$  increases, a level might cross from positive to negative or vice versa. When this happens, the gauge field is regarded to have a net topological charge  $|Q| = 1$ . Then the overlap determinant is exactly zero by construction. This definition of lattice topology and zero mode do depend on, for instance, the Wilson parameters  $r$  and  $m_0$ . However, the zero eigenvalue is exact, independent of the lattice spacing  $a$  and volume  $V$ .

**Current figure:**

Figure image:

Figure coordinates:  
(x = 118, y = 74, width = 374, height = 262)

**Select the boundary**

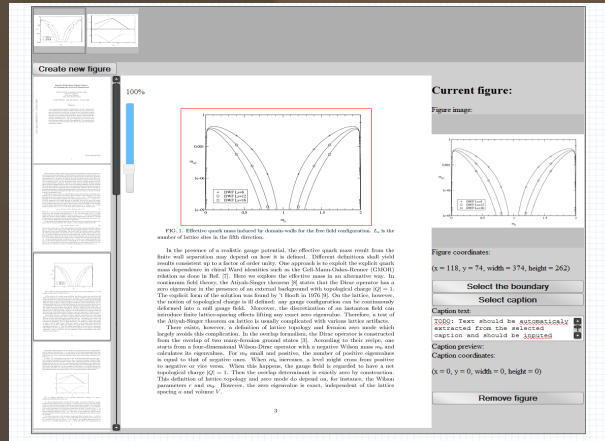
**Select caption**

**Caption text:**  
TODO: Text should be automatically extracted from the selected caption and should be imputed
G-0

**Caption preview:**  
**Caption coordinates:**  
(x = 0, y = 0, width = 0, height = 0)

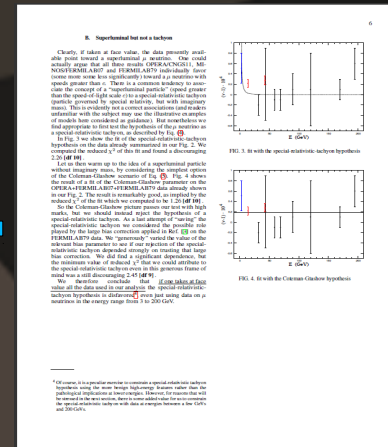
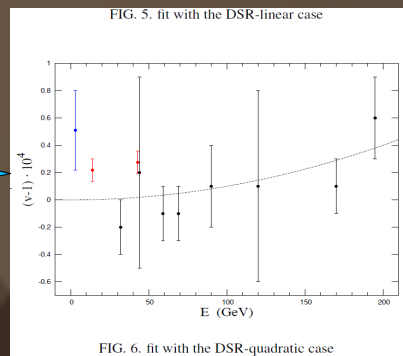
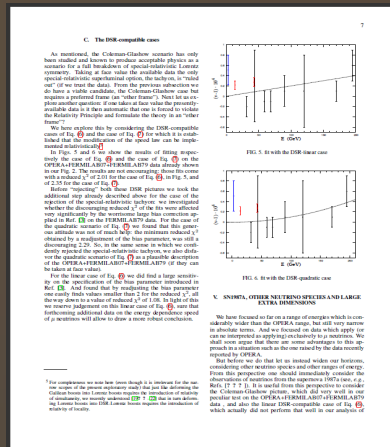
**Remove figure**

# Extraction based on metadata



- User has already provided position of figures in the document, we need to produce graphical files and upload them

# *Figures from scientific publications*



Extracted from

Extracted from

Figure 1  Describes the same data

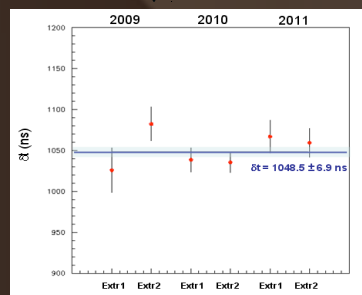


Figure 2 (extracted from different publication)



*Questions ?*